10/3/10/93 W.B. D

2/15

SANDIA REPORT

SAND92—2651 • UC—704
Unlimited Release
Printed February 1993

Moisture Permeation of Environmental Seals Used in Weapons

Kenneth T. Gillen, Peter F. Green

Prepared by
Sandia National Laboratories
Albuquerque, New Mexico 87185 and Livermore, California 94550
for the United States Department of Energy
under Contract DE-AC04-76DP00789

Issued by Sandia National Laboratories, operated for the United States Department of Energy by Sandia Corporation.

Available to DOE and DOE contractors from
Office of Scientific and Technical Information
PO Box 62
Oak Ridge, TN 37831

Prices available from (615) 576-8401, FTS 626-8401

Available to the public from
National Technical Information Service
US Department of Commerce
5285 Port Royal Rd
Springfield, VA 22161

NTIS price codes
Printed copy: A03
Microfiche copy: A01

SAND92-2651
Unlimited Release
Printed February, 1993

Distribution
Category UC-704

SAND--92-2651

DE93 008489

MOISTURE PERMEATION OF ENVIRONMENTAL SEALS USED IN WEAPONS

Kenneth T. Gillen and Peter F. Green
Sandia National Laboratories
Albuquerque, NM 87185

ABSTRACT

To allow more reliable estimates to be made of the amount of water that permeates through weapon environmental seals, we have generated extensive water permeability coefficient data for numerous o-ring materials, including weapon-specific formulations of EPDM, butyl, fluorosilicone and silicone. For each material, data were obtained at several temperatures, ranging typically from 21°C to 80°C; for selected materials, the effect of relative humidity was monitored. Two different experimental techniques were used for most of the measurements, a permeability cup method and a weight gain/loss approach using a sensitive microbalance. Good agreement was found between the results from the two methods, adding confidence to the reliability of the measurements. Since neither of the above methods was sufficiently sensitive to measure the water permeability of the butyl material at low temperatures, a third method, based on the use of a commercial instrument which employs a water-sensitive infrared sensor, was applied under these conditions.

TABLE OF CONTENTS

ABSTRACT 1

INTRODUCTION 3

EXPERIMENTAL 3
- Materials 3
- Permeability Cup Measurements 4
- Weight Change Measurements 5
- Modulated Infrared Sensor Technique 6

RESULTS AND DISCUSSION 6

CONCLUSIONS 19

REFERENCES 22

DISTRIBUTION 23

INTRODUCTION

A long-term and continuing need for most weapon systems is the development of quantitative methods for estimating the lifetime water ingress past the environmental o-ring seals. Two components contribute to water ingress, permeation through the seals and leakage around the seals. We have shown in recent reports (Gillen, 1987, 1990) that, if the permeation contribution can be estimated, the lifetime integrated leakage can often be estimated (for nitrogen backfilled weapons) by analysis of the argon concentration found in the weapon during surveillance. Estimating the permeation contribution requires estimates of the weapon's environmental history (temperature and humidity versus time) plus reliable, temperature-dependent values for the water permeability coefficient appropriate to the environmental sealing material. For many of the sealing materials used in weapons, reliable water permeability coefficients are not available, even at ambient temperature. As an example, no measurements of any kind have been published for the newly developed EPDM material being used on the W88 and being considered for the W89. As shown below, literature values for other EPDM and butyl materials show significant scatter (up to two orders of magnitude). Some of this scatter can be attributed to the expected variations caused by formulation differences since there are literally hundreds of EPDM and butyl formulations available commercially. But the main source of the scatter comes from the fact that water permeation measurements can be difficult with many possible sources of experimental error, precluding confident use of such data. Given the importance of having reliable water permeability coefficients, P, for estimating water ingress into weapons, the main goals of this study were to obtain and compare temperature-dependent P values derived from two different experimental approaches for several of the most important o-ring formulations used on past and present weapons and/or likely to be used on future systems. The first technique invoked the use of water vapor permeability cups (ASTM Standard E96-90). This simple approach utilizes a disk of the material covering a reservoir as a vapor barrier. By creating a known differential water vapor concentration on the two sides of the barrier and following the overall weight change of the apparatus, P can be calculated. The second technique follows weight changes versus time for samples suspended from a sensitive electronic microbalance after "instantaneous" changes in the humidity environment surrounding the sample. These experiments are more difficult to perform but offer the advantages of taking less time and of yielding values for both the water diffusion constant, D and the water solubility coefficient, S of the material, the product of which equals P.

EXPERIMENTAL

Materials

The materials used in this study include common o-ring formulations, many of which are the precise materials used in past and present weapon systems. Table 1 lists the compound number, the manufacturer, the polymer type and the formulation density. Except for the last two materials in the Table, the formulations are proprietary and therefore unavailable. The final two entries were special EPDM materials, formulated

for the Allied-Signal Kansas City Plant; their formulations are shown in Table 2. All materials were obtained as 15 cm by 15 cm compression molded sheets of various thicknesses ranging from approximately .06 cm to .21 cm.

Table 1. Materials used in study

Compound Number	Manufacturer	Polymer Type	Density, g/cc
B612-70	Parker	Butyl	1.18
E740-75	Parker	EPDM	1.12
E515-80	Parker	EPDM	1.24
E692-75	Parker	EPDM	1.26
S604-70	Parker	Silicone	1.20
LS-53		Fluorosilicone	1.42
S041-70		Fluorosilicone	1.44
SR793B-80	Stillman	EPDM	1.14
A-70		EPDM	1.14

Table 2. SR-793B/80 and A70 Formulations

SR-793B/80		A-70	
Constituent	pph	Constituent	pph
Dupont Nordel 1440	100	Dupont Nordel 1440	100
Zicstick 85	5	Cis 1,4 polybutadiene	5
N-990 carbon black	40	N-990 carbon black	40
N-539 carbon black	25	N-539 carbon black	25
Flectol H	2	Vanox ZMTI	2
DiCup 40C	12	Varox 40C	8
SR-350	10	Rocryl 910	5
		Zinc oxide	5

Permeability Cup Measurements

Fisher/Payne permeability cups no. 13-338 were used for these studies. This apparatus allows a disk of the material being studied to be clamped tightly over a reservoir cup. By creating a known differential water vapor concentration on the two sides of the barrier and following the overall weight change of the apparatus, water permeability coefficients can be calculated. A circular cutter was used to extract 6.35 cm diameter disks of each material. The average thickness of each disk was estimated, usually by weighing the disk and calculating the thickness based on the known (from density gradient column measurements) density of the disk (see Table 1). For most experiments, approximately 10-12 cc of distilled water was added to the cup (~75% filled), followed by installation of the rubber disk, using an extremely small amount of Krytox grease on the cup flange metal surface. Although the grease can be helpful in

sealing the edges of the sample, a minimum amount is used to reduce the chance of grease exuding out the edges of the seal, which could lead to an anomalous loss of weight. The cup was then typically placed on a porcelain plate in a desiccator (activated molecular sieve desiccant is placed below the plate). The sealed desiccator was next placed in a controlled temperature environment (e.g., air-circulating oven), which was continuously monitored by a thermocouple located adjacent to the dessicator. For this arrangement, one side of the material disk (the side covering the cup of water) was exposed to 100% R.H. at the selected temperature whereas the other side of the disk was essentially at 0% R.H. For several experiments, water saturated with NaCl was placed in the cup; this corresponded to 75±1% R.H. conditions. Occasionally, at the highest temperatures used in the study (typically at 60°C and above), the water-filled permeation cups were placed directly in the oven. In these instances, the water vapor pressure on the outside of the cups was estimated to be 0.7±0.2 cmHg, which was subtracted from the internal value (greater than 14 cmHg) to obtain the differential vapor pressure.

Periodic weighing (typically days to weeks apart dependent on the rate of weight loss) of the permeation cup apparatus were carried out as follows. A 100 g standard weight was carefully weighed to 0.1 mg on an enclosed Mettler AE163 electronic balance; this served to check the operation of the balance and as a reference weight for the weighing procedure. Then, as quickly as practical, the dessicator was removed from its temperature environment, the permeation cup removed, weighed, replaced in the dessicator and the dessicator replaced in the oven. The periodic weighing procedure was repeated a minimum of 5 times until reasonably constant rates of weight loss from weighing to weighing were found. For conditions where fairly rapid weight loss occurred (greater than ~10 mg/week), scatter in the rate of weight loss was typically less than ±10%. For conditions with lower rates of weight loss (low permeability materials at low temperatures), larger scatter was observed, necessitating the collection of data over extended time periods (many months).

Weight Change Measurements

Measurements of the weight change (gain and loss) were performed as a function of time using a Cahn 1000 microbalance. The complete weighing apparatus was contained in a temperature-controlled, sealed chamber. For weight gain measurements, the sample was initially placed on the balance in a dry, desiccated part of the chamber and the chamber brought to temperature equilibrium. At the start of an experiment, two valves simultaneously closed off the dessicator section of the chamber and exposed the sample region to a saturated solution of sodium chloride and water (corresponds to 75% R.H. for the temperatures currently used). Within a few minutes, the sample region reached 75% R.H. as measured by a humidity sensor located near the sample. The weight gain was then monitored as a function of time using the microbalance. Temperature was monitored by thermocouples placed in the salt solution and in the environment near the sample. In some experiments, water desorption (weight loss) measurements were made after the sorption experiment was complete (e.g., after the sample stopped gaining weight during the sorption experiment). At the beginning of the water desorption phase of the experiment, the valving was used to quickly change the

sample environment from 75% R.H. to dry conditions. Weight loss was then followed versus time using the microbalance.

Modulated Infrared Sensor Technique

At low temperatures, the butyl material has an extremely low water permeability coefficient. Neither the permeation cup method nor the weight change approach was sufficiently sensitive to obtain accurate values for P under these conditions. Measurements were carried out by Mocon Modern Controls, Inc. at 23°C using an instrument based on the ASTM Standard F 1249-89. Similar to the permeation cup method, a sheet of the material separates a high humidity region (100% R.H. for our experiments) from a low humidity region. A dry air stream (less than 1 ppm water vapor) flows past the low humidity side of the sample to an infrared sensor which quantifies (based on known, calibrated materials) the concentration of water vapor which permeates through the sample.

RESULTS AND DISCUSSION

The three experimental techniques used in the current study are based on two different types of experiments, steady-state and time-dependent. The first two approaches (permeation cup and infrared sensor techniques) take advantage of the fact that P can be obtained from the one dimensional, steady-state transport of moisture vapor across a plane sheet of cross-sectional area A and thickness L. The validity of these approaches relies on (1) the water diffusion coefficient D being independent of water concentration in the material and (2) the existence of a linear relationship between the external water vapor pressure p and the corresponding equilibrium dissolved concentration, i.e., $C = Sp$ where S is the solubility coefficient. The third approach (weight gain/loss) directly determines values for D and S by monitoring the time-dependent weight change of a thin sheet of material (thickness 2ℓ) placed in an environment where the concentration at the faces of the film is constant. The permeability coefficient P is then given by the product of D and S.

For the steady-state techniques, assume that we have a sheet of elastomer of thickness L and a coordinate system with $x = 0$ at one surface of the sheet and $x = L$ at the opposite surface. If the water concentrations at the two surfaces are c_1 (at $x = 0$) and c_2 (at $x = L$) then the rate of water transfer per unit area is (Crank, 1975)

$$J = -D\, dc/dx = D\,(c_1 - c_2)/L \qquad (1)$$

Although the concentrations c_1 and c_2 are in general unknown, the water vapor pressures on the two sides of the sample, p_1 and p_2 can be estimated. Assuming Henry's Law, which predicts a linear relationship between the concentration and the vapor pressure ($c = Sp$), where S is the water solubility coefficient, one obtains the following relationship for the steady-state flow of moisture through the sample

$$F = AJ = ADS\,(p_1 - p_2)/L = AP\,(\Delta p)/L \quad (2)$$

where P has been substituted for D times S and $\Delta p = p_1 - p_2$. Thus P can be obtained from

$$P = FL/(A\Delta p) \quad (3)$$

where A, L and Δp are known and F is determined experimentally.

For permeation cup measurements, F is obtained when water weight loss data reach steady-state conditions (e.g., weight loss is linear with time). Typical permeation cup weight loss data for conditions of relatively high weight loss (~34 mg/week) are shown in the left-hand plot of Fig. 1 (for convenience, the first point in the steady state region is taken as time zero). These data are for a 0.094 cm thick sample of the SR793B-80 material exposed at 62.4°C with water (100% R.H.) in the cup and ~0% R.H. on the opposite side of the sample. The steady-state weight loss rate comes from the slope of the line through the results. Even though the results appear to be extremely linear, individual points lie up to a couple of mg above or below the line. This deviation, which comes from a combination of random and systematic errors, has minimal effect when the rate of weight loss is relatively fast but becomes more significant for lower rates of weight loss. The right-hand plot of Fig. 1, for instance, shows data for this same material at 21°C with saturated NaCl solution (75% R.H.) in the permeation cup. In this case the weight loss is ~ 2.5 mg/week and the deviations from the straight line are more obvious. This means that data must be taken for a fairly long time period to derive reliable values for this slope.

The weight loss rates obtained from the permeation cup experiments are summarized in Table 3 as a function of the following experimental variables- material, material thickness (L), temperature (T) and the internal, external and differential water vapor partial pressures (p_i, p_e and Δp, respectively) appropriate to the sample.

Table 3. Permeability Cup Results

Material	L	T,	p_i,	p_e,	Δp	Wt loss rate	P
	cm	°C	cmHg	cmHg	cmHg	g/h	ccSTP/cm/s/cmHg
SR793B-80	0.094	41.1	5.86	0.7	5.16	9.50E-5	5.95E-8
	0.094	21	1.87	0	1.87	2.05E-5	3.55E-8
	0.094	45.6	7.41	0	7.41	1.60E-4	6.98E-8
	0.094	43.7	6.71	0	6.71	1.33E-4	6.41E-8
	0.094	41.1	4.4*	0.7	3.7	6.14E-5	5.36E-8
	0.094	21	1.4*	0	1.4	1.47E-5	3.38E-8
	0.094	45.6	5.6*	0	5.6	1.13E-4	6.53E-8
	0.094	43.7	5.0*	0	5.0	9.2E-5	5.91E-8

Table 3. Continued

Material	L cm	T, °C	p_i, cmHg	p_e, cmHg	Δp cmHg	Wt loss rate g/h	P ccSTP/cm/s/cmHg
SR793B-80	0.094	41.1	0	5.86	5.86	1.08E-4	5.96E-8
	0.208	62.4	16.7	0	16.7	2.05E-4	8.83E-8
	0.208	62.4	16.7	0	16.7	2.53E-4	1.09E-7
	0.208	43.7	6.71	0	6.71	6.1E-5	6.54E-8
E740-75	0.17	80.0	35.5	0.7	34.8	8.66E-4	1.46E-8
	0.17	41.3	5.9	0.7	5.2	5.29E-5	5.98E-8
	0.17	21	1.87	0	1.87	1.15E-5	3.62E-8
	0.17	62.4	16.7	0	16.7	2.53E-4	8.9E-8
	0.15	62.4	16.7	0	16.7	2.93E-4	9.1E-8
	0.15	62.4	16.7	0	16.7	3.47E-4	1.08E-7
	0.15	43.7	6.71	0	6.71	8.85E-5	6.84E-8
	0.071	21	1.87	0	1.87	2.73E-5	3.59E-8
	0.071	43.7	6.71	0	6.71	1.8E-4	6.58E-8
	0.17	62.4	16.7	0	16.7	2.67E-4	9.39E-8
E515-80	0.146	62.4	16.7	0	16.7	2.81E-4	8.49E-8
	0.146	62.4	16.7	0	16.7	3.24E-4	9.79E-8
	0.146	43.7	6.71	0	6.71	6.95E-5	5.23E-8
	0.082	21	1.87	0	1.87	1.77E-5	2.69E-8
	0.082	43.7	6.71	0	6.71	1.24E-4	5.24E-8
E692-75	0.07	21	1.87	0	1.87	2.59E-5	3.36E-8
	0.07	45.6	7.41	0	7.41	1.98E-4	6.47E-8
	0.07	43.7	6.71	0	6.71	1.65E-4	5.95E-8
	0.203	59.9	14.9	0	14.9	1.92E-4	9.04E-8
	0.203	60.3	15.1	0.7	14.4	2.08E-4	1.01E-7
	0.203	80.3	35.9	0.7	35.2	6.81E-4	1.36E-7
	0.203	80.2	35.8	0.7	35.1	6.76E-4	1.35E-7
A-70	0.198	59.9	14.9	0	14.9	2.06E-4	9.46E-8
	0.198	60.3	15.1	0.7	14.4	2.28E-4	1.08E-7
	0.198	80.3	35.9	0.7	35.2	7.76E-4	1.51E-7
	0.198	80.2	35.8	0.7	35.1	7.61E-4	1.48E-7
B612-70	0.144	59.9	14.9	0	14.9	4.86E-5	1.62E-8
	0.144	60.3	15.1	0.7	14.4	5.6E-5	1.93E-8
	0.144	80.3	35.9	0.7	35.2	2.65E-4	3.75E-8
	0.144	62.4	16.7	0	16.7	4.86E-5	1.40E-8
	0.144	62.4	16.7	0	16.7	6.77E-5	2.02E-8
S041-70	0.178	44.2	6.9	0	6.9	1.63E-3	1.21E-6
	0.178	21	1.87	0	1.87	3.7E-4	1.22E-6
	0.178	59.9	14.9	0	14.9	3.0E-3	1.24E-6
LS-53	0.198	44.2	6.9	0	6.9	1.5E-3	1.49E-6
	0.198	59.9	14.9	0	14.9	3.32E-3	1.53E-6
	0.198	21	1.87	0	1.87	4.2E-4	1.54E-6

Table 3. Continued

Material	L cm	T, °C	p_i, cmHg	p_e, cmHg	Δp cmHg	Wt loss rate g/h	P ccSTP/cm/s/cmHg
S604-70	0.208	44.2	6.9	0	6.9	2.02E-3	2.11E-6
	0.208	21	1.87	0	1.87	6.9E-4	2.66E-6
	0.208	59.9	14.9	0	14.9	4.0E-3	1.93E-6

* saturated NaCl solution in cup (75% R.H.)

By converting the weight loss rates in Table 3 (g/h) to ccSTP/s and noting that A = 10 cm^2 for our experimental setup, eq. (3) can now be used together with the data of Table 3 to calculate the water permeability coefficients, P; the final column of the Table summarizes the results.

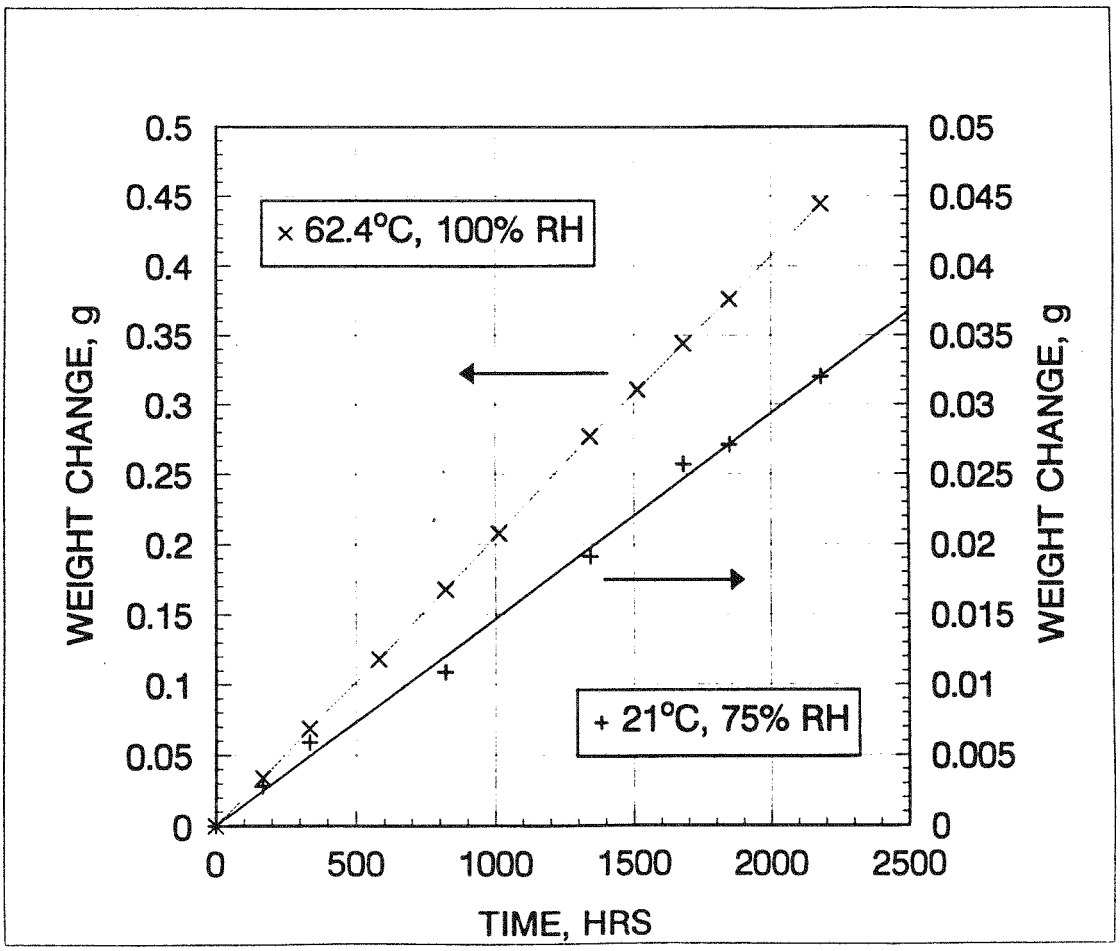

Figure 1. Typical permeation cup weight loss data under the two indicated conditions for the SR793B-80 material.

Because of the relative simplicity of the permeation cup approach, one might expect very little experimental scatter in the data. In fact, the results for repeated determinations under "identical" temperature and Δp conditions (e.g., E740-75 and E515-80 at 21°C, 43.7°C and 62.4°C, B612-70 at 62.4°C) indicate data scatter may be up to ± 20%. In the recent ASTM Standard E 96-90, which discusses the permeation cup method, reference is made to an interlaboratory test (fifteen laboratories participated) comparing the reproducibility of results for four different materials. For the water method (distilled water in cup, apparatus in dessicator at room temperature), the coefficient of variation (100 times the standard deviation divided by the mean) was determined to be ~20% for all four samples.

We therefore conclude that the values of P derived in Table 3 are precise to better than ±20%. Errors come from many possible sources. Increases in the apparent value of P above its actual value will occur due to (1) small leaks between the sample and its sealing surface along the cup flange, (2) slight swelling of the sample at elevated temperatures (caused by excess pressure inside cup) which slightly increases the permeation area and decreases the sample thickness, (3) permeation through the edges of the sample, and (4) weight losses due to aging, loss of lubricants, etc. Decreases in the apparent value of P occur whenever Δp is less than the expected value caused by a number of possible effects such as (1) a reduced partial pressure at the cup exposed surface of the sample due to a gradient in water vapor pressure in the air layer separating this surface and the water and (2) the existence of a non-zero vapor pressure in the dessicator. A temperature difference between the thermocouple and the sample can lead to errors in either direction. These and other sources of error have been described in the literature (Abrams, 1936; Newns, 1950).

Butyl rubbers are known to have very low water permeability coefficients. For our butyl material (B612-70), we were unable to generate reliable results using the permeation cup method at temperatures below 60°C, even for our thinnest specimens (~0.06 cm thick). We therefore obtained 23°C results (Δp = 2.11 cmHg) for two samples of B612-70 using the Modulated Infrared Sensor Technique. For the first sample, whose thickness was 0.0673 cm, the measured water flux was 5.17×10^{-8} ccSTP/cm^2/s, resulting in a P of 1.65×10^{-9} ccSTP/cm/s/cmHg. The second sample (L=0.0685 cm) had a flux of 5.06×10^{-8} ccSTP/cm^2/s, leading to an almost identical value for P (1.64×10^{-9} ccSTP/cm/s/cmHg).

For the experiments involving the time-dependent weight gain of water by a film of the elastomer surrounded by a constant humidity environment (vapor pressure p), consider the film to be of thickness 2ℓ, its faces being located at $+\ell$ and $-\ell$ and x = 0 in the center of the film. Assuming that the equilibrium water concentration at the surfaces C_1 (equal to Sp, as usual) is established instantaneously, standard treatments (Crank, 1975; Comyn, 1985) give the following time-dependent expression for the concentrations C within the film

$$\frac{C}{C_1} = 1 - \frac{4}{\pi}\sum_{n=0}^{\infty}\frac{(-1)^n}{2n+1}\exp\left(\frac{-D(2n+1)^2\pi^2 t}{4\ell^2}\right)\cos\left(\frac{(2n+1)\pi x}{2\ell}\right) \quad (4)$$

This equation can be integrated to give the ratio of the time-dependent mass uptake M_t over the mass uptake at equilibrium, M_∞

$$\frac{M_t}{M_\infty} = 1 - \sum_{n=0}^{\infty}\frac{8}{(2n+1)^2\pi^2}\exp\left(\frac{-D(2n+1)^2\pi^2 t}{\ell^2}\right) \quad (5)$$

At short times this equation can be approximated by

$$\frac{M_t}{M_\infty} = 4\left(\frac{Dt}{\pi\ell^2}\right)^{\frac{1}{2}} \quad (6)$$

This equation can be used on the early weight gain results out to M_t/M_∞ ~0.55 (see Fig. 4.6 of Crank, 1975) to extract values for D; values of S are obtained from the measured values of M_∞ and P as the product of D and S. This same equation applies to the early stages of weight loss measurements so the analysis is identical except that M_t and M_∞ refer to time-dependent weight loss and the total mass loss at equilibrium, respectively.

Figures 2 and 3 show sorption (weight gain) results for an 0.08 cm thick sample of the E740-75 material at 24°C and 75% R.H. conditions (p = 1.68 cmHg). M_t/M_∞ is plotted versus the square root of time with Fig. 2 showing the data out to saturation and Fig. 3 highlighting the early-time region. From the slope of $4.6 \pm 0.25 \times 10^{-3}$ $s^{-1/2}$ found for the linear region of the results (Fig. 3), eq. (6) leads to a D value of $2.7 \pm 0.3 \times 10^{-8}$ cm^2/s. Since M_∞ was found to be 230 μg for a sample that initially weighed 0.168 g and the density of this material is 1.12 g/cc (Table 1), S can be calculated to be 1.14 ccSTP/cc/cmHg. Desorption (weight loss) measurements for this sample gave essentially identical results.

In general, two to three experiments (sorption and/or desorption) were run at a given temperature for each sample studied. Based on repeated runs, estimated uncertainties are ~±25% for values of D and S. One of the largest sources of error comes from the long-term drift in the microbalance output since most experiments took several days to complete. This drift typically causes the errors in D and S to go in opposite directions. Due to such compensation effects, the uncertainties in P (the product of D and S) are also estimated to be ~±25%. Table 4 reports the average values for D, S and P derived from the current sorption/desorption experiments. The results in the Table show that the large differences found in the values of P between the three EPDM materials (first three materials) and the silicone and fluorosilicone materials (bottom three) is due to the two order of magnitude differences in diffusion coefficients.

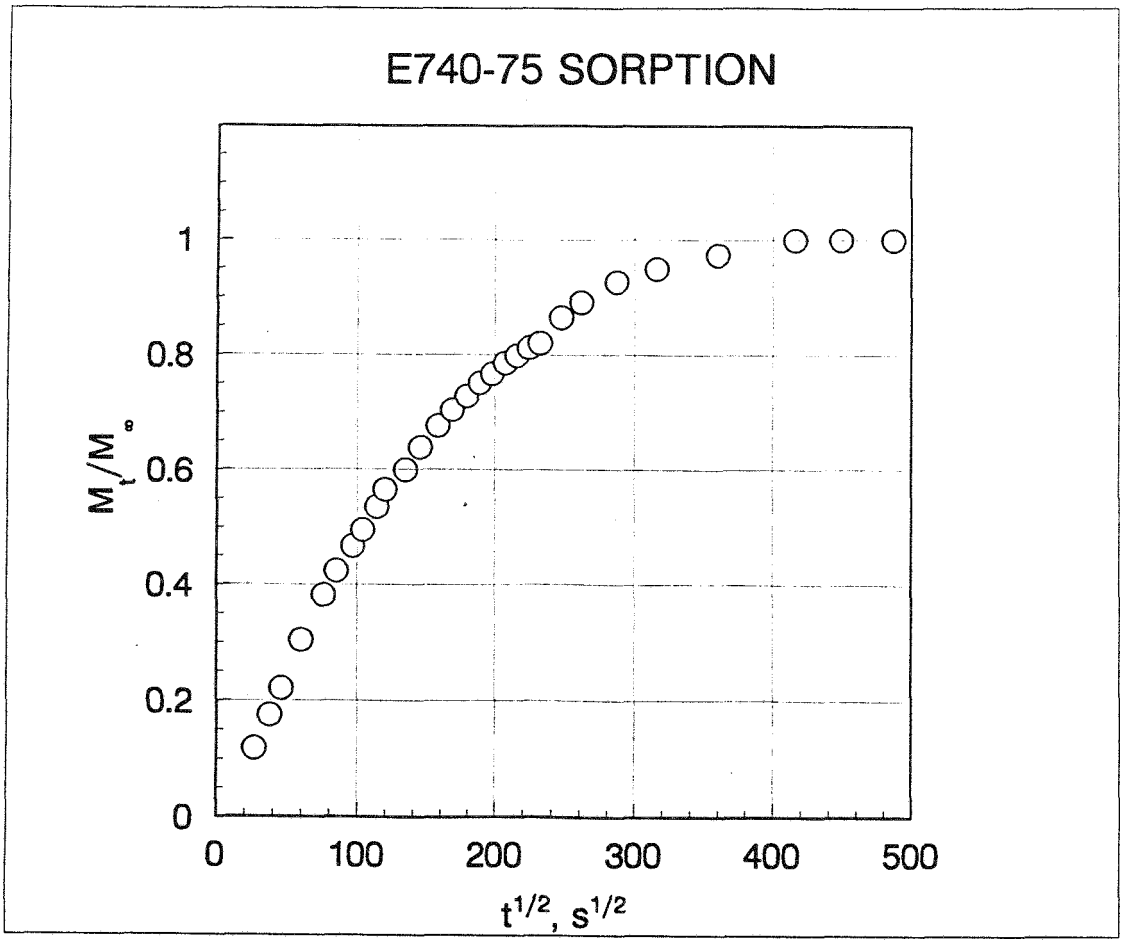

Figure 2. Typical microbalance weight gain results for E740-75 at 24°C and 75% R.H. The weight gain at time t over the saturation value (M_t/M_∞) is plotted versus $t^{1/2}$.

Table 4. Sorption/Desorption Results

Material	T °C	D cm^2/s	S ccSTP/cc/cmHg	P ccSTP/cm/s/cmHg
SR793B-80	24	2.6E-8	0.86	2.2E-8
	50	1.0E-7	0.8	8.0E-8
E740-75	24	2.7E-8	1.14	3.1E-8
	37	3.3E-8	1.1	3.6E-8
	51	7.0E-8	0.9	6.3E-8
	56	7.0E-8	1.4	9.8E-8
E692-75	40	9.0E-8	0.6	5.4E-8
	50	6.9E-8	0.84	5.8E-8
	55	1.4E-7	0.6	8.4E-8
S604-70	35	2.0E-6	1.04	2.1E-6
LS-53	35	1.1E-6	1.19	1.3E-6
S041-70	35	1.7E-6	0.9	1.5E-6

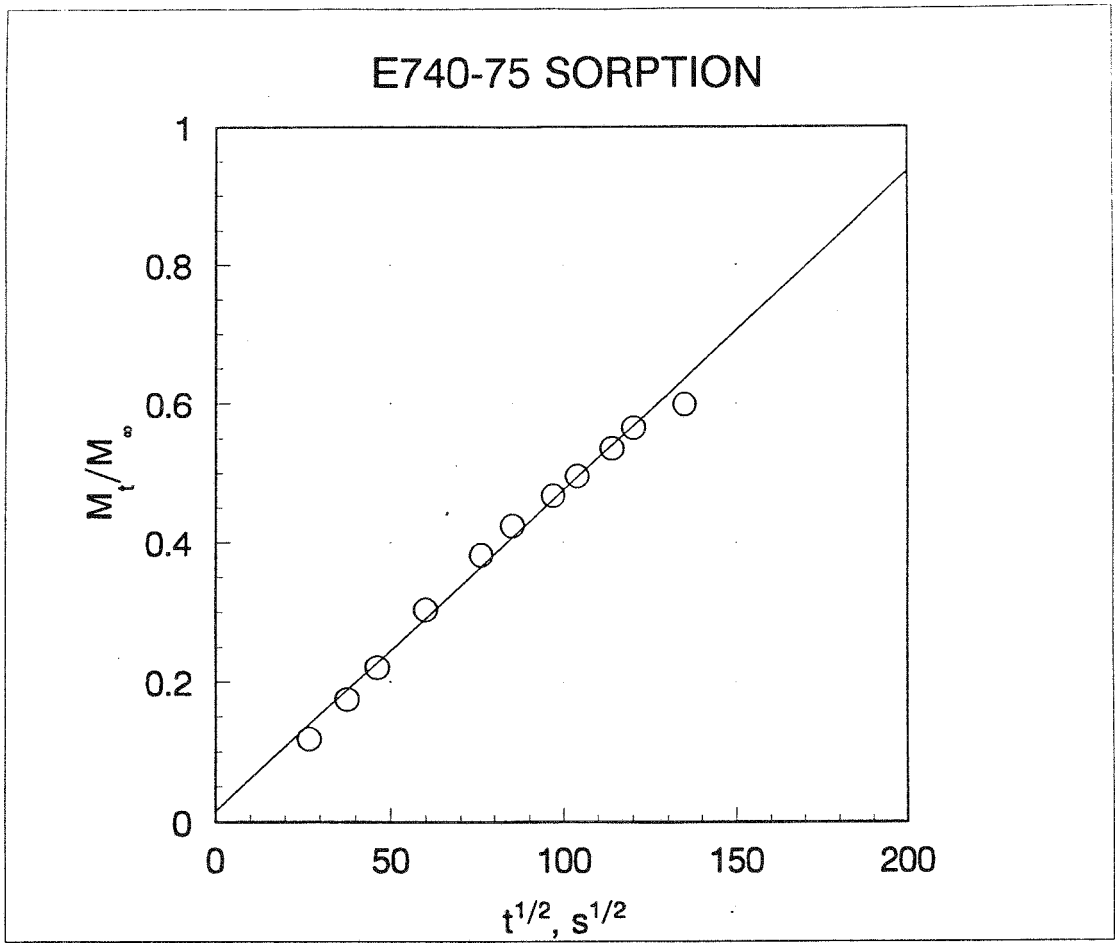

Figure 3. Detail of the Fig. 2 data showing the linear region used to obtain an estimate of the diffusion coefficient.

We now combine the permeability coefficient results from the three experimental techniques in logarithmic plots of P versus inverse temperature (Figs. 4-11). For such plots, linear behavior corresponds to the Arrhenius temperature dependence often found for permeability coefficients, in which

$$P \propto \exp(-E_a/RT) \tag{7}$$

where R is the gas constant and E_a is the Arrhenius activation energy.

Figure 4 shows results for the SR793B-80 EPDM material from permeation cup measurements at both 100% R.H. and 75% R.H. and 75% R.H. microbalance measurements. The first observation to make is that, although there might be a slight effect of relative humidity for the permeation cup results (P at 75% R.H. may be 10% lower than at 100% R.H.), within the experimental uncertainties of ~±20%, the results

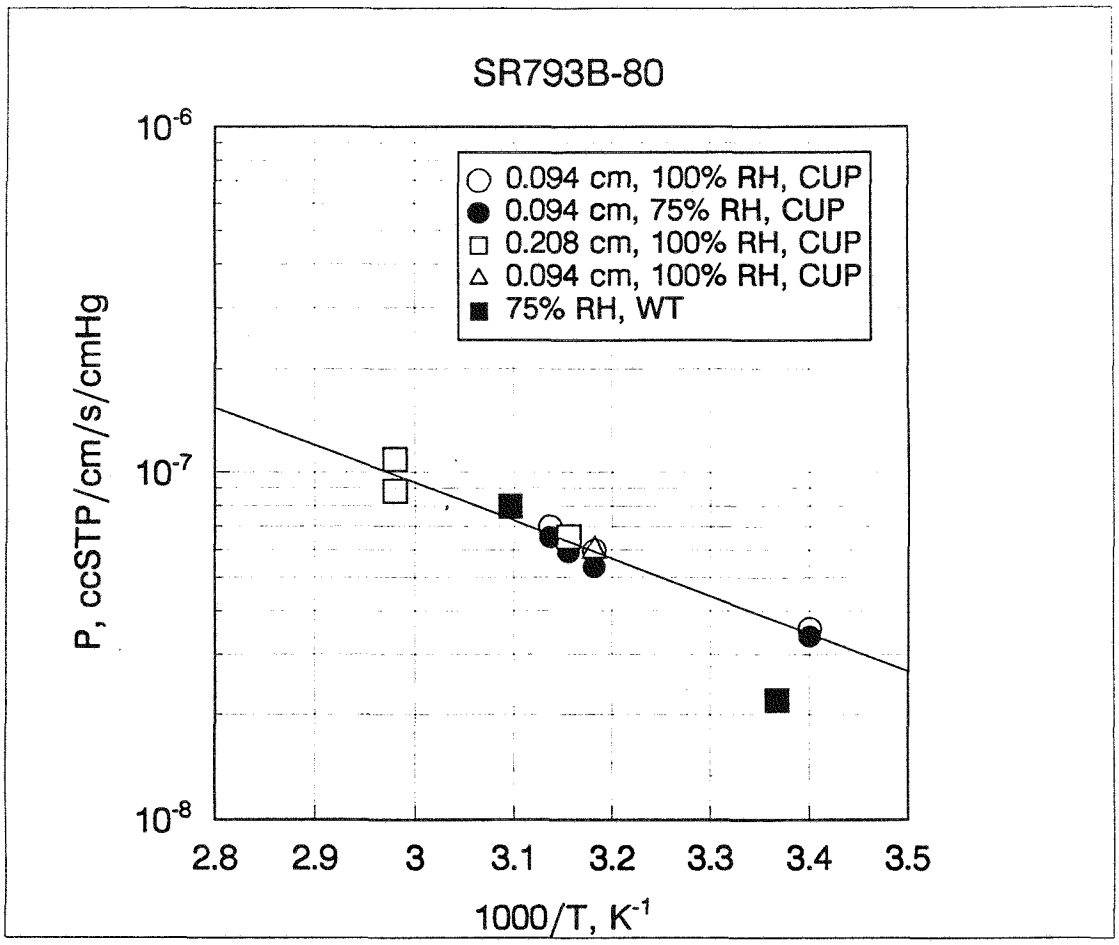

Figure 4. Permeability coefficient results for the SR793B-80 material plotted versus inverse absolute temperature.

can be considered identical. A reasonable straight line can be drawn through the permeation cup results, indicating Arrhenius behavior within the experimental uncertainty; the slope of the line corresponds to an E_a of 5.0 kcal/mol. The sorption/desorption result at 50°C is in excellent agreement with the permeation cup results. Although the 24°C result is somewhat lower than the permeation cup line, it is still in reasonable agreement considering its estimated 25% experimental uncertainty and the possibility that it could be slightly lower due to the reduced (75% versus 100%) R.H. conditions.

Figures 5 and 6 summarize our measurements on two other EPDM materials (E740-75 and E692-75) where both the permeation cup and sorption/desorption techniques were applied. Again, we find reasonable agreement between the two techniques. Straight lines drawn through the permeation cup results correspond to

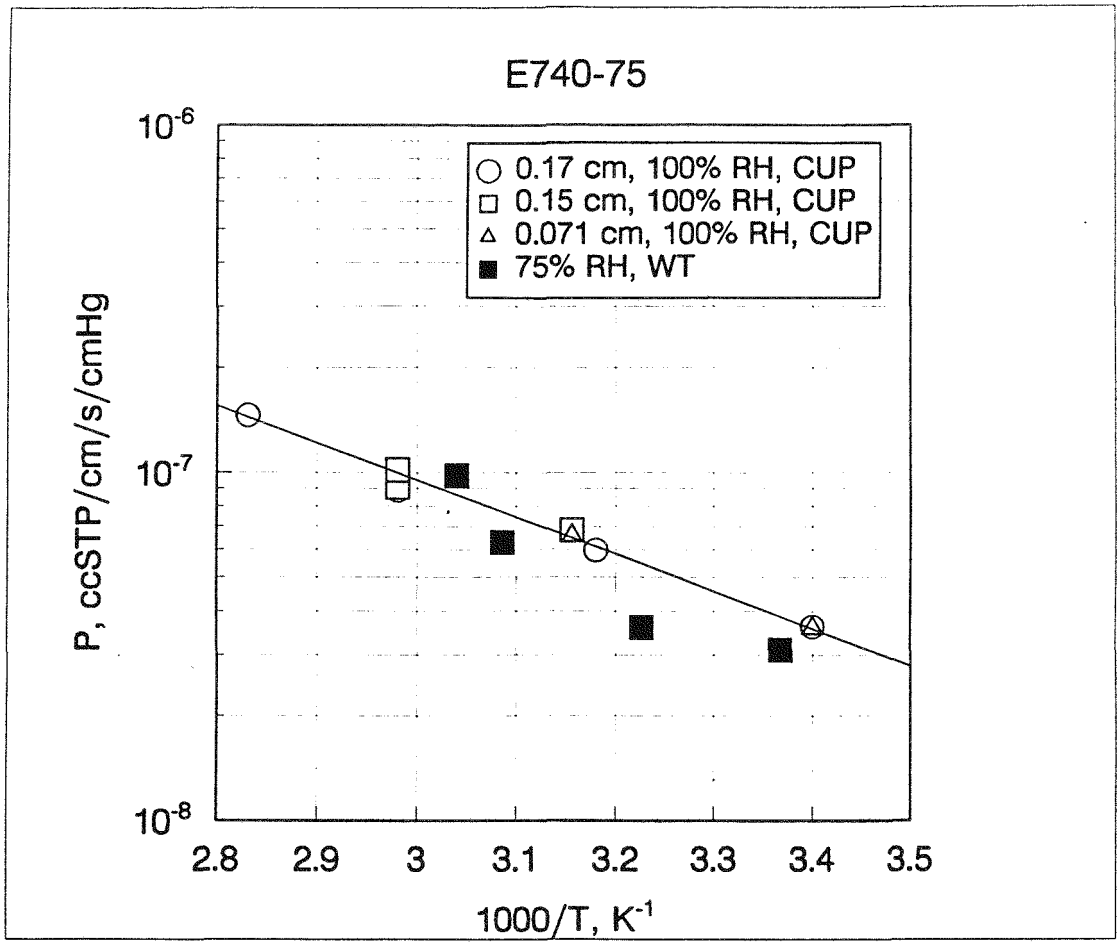

Figure 5. Permeability coefficient results for the E740-75 material plotted versus inverse absolute temperature.

activation energies of 4.9 and 5.0 kcal/mol, respectively. A literature result, which exists for the E692-75 material (Parker, 1982), is also plotted in Fig. 6.

Figures 7 and 8 show our permeation cup results for the two remaining EPDM materials, E515-80 and A-70 (the lines correspond to activation energies of 5.7 and 4.6 kcal/mol, respectively), plus literature results (Helander, 1984) for E515-80. The results for A-70, though limited to only a few high temperature measurements, are interesting since 5 pph cis 1,4 polybutadiene was added to this formulation as a means of producing a slight reduction in rubber hardness relative to the SR793B-80 formulation (see Table 2). Like many rubbers, literature values for the water permeability coefficient of polybutadiene vary tremendously. For instance, one reported result at 37.5°C (Barrie, 1968) is 5.07×10^{-7} ccSTP/cm/s/cmHg; a more recent result (Rogers, 1985) at 25°C is 4.7×10^{-8} ccSTP/cm/s/cmHg. If the former result was appropriate, one might expect that the addition of 5 pph polybutadiene to the EPDM formulation would significantly raise

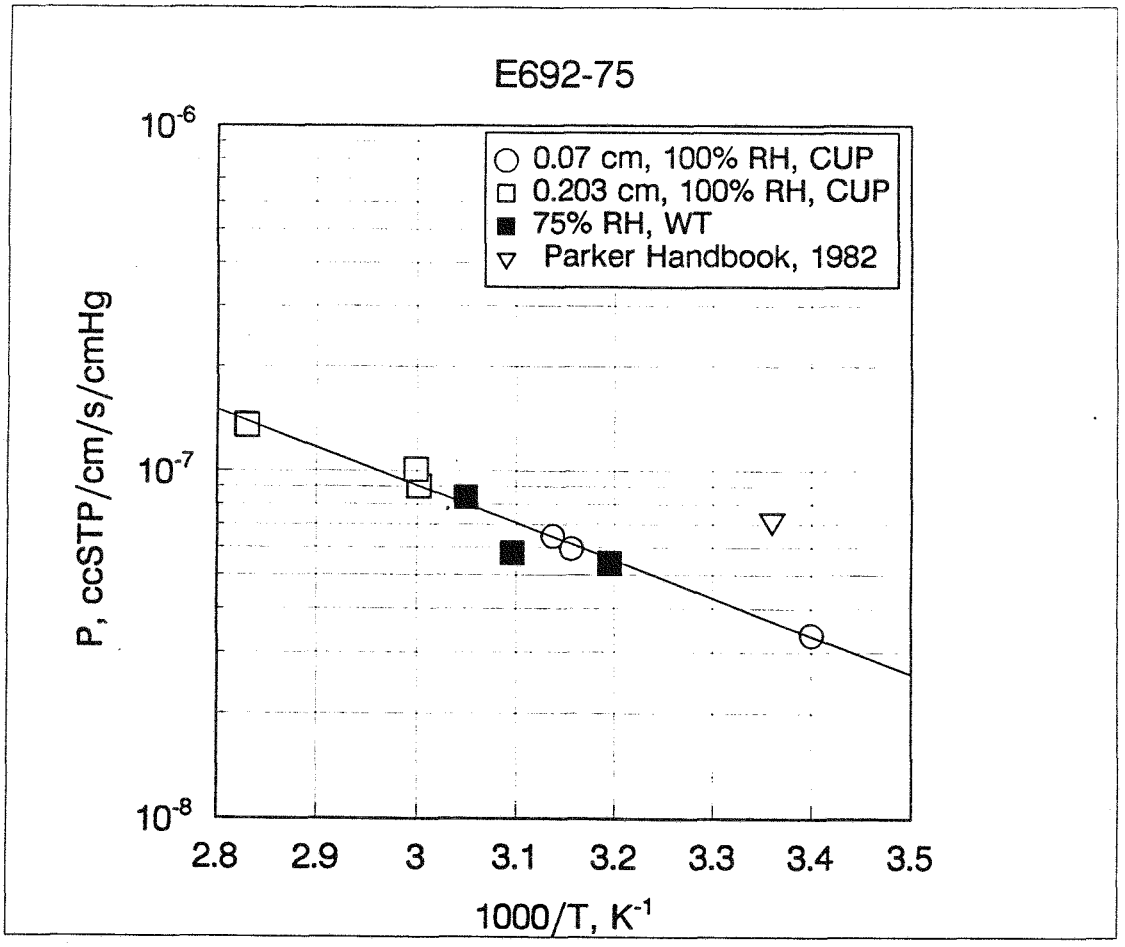

Figure 6. Permeability coefficient results for the E692-75 material plus a literature value plotted versus inverse absolute temperature.

the water permeability coefficient. In fact, the results for the A-70 formulation are quite similar to the other EPDMs studied, implying either that the more recent polybutadiene result is correct or that little sensitivity to formulation changes is found for EPDMs.

The excellent agreement between the five EPDM formulations currently being studied is summarized in Fig. 9, where the five lines through the permeation cup results in Figs. 4-8 are shown on the same plot. Given this agreement and, in the absence of actual data, a conservative assumption for the room temperature (21°C) water permeability coefficient for any other EPDM material being used in a weapon system would be $3.5\pm1\times10^{-8}$ ccSTP/cm/s/cmHg. To obtain values at other temperatures of interest, an activation energy of 5.1±0.5 kcal/mol would be an appropriate estimate.

Figure 10 summarizes our results (permeation cup at temperatures ranging from ~60°C to 80°C and infrared detector at 23°C) for the butyl B612-70 material. Using the

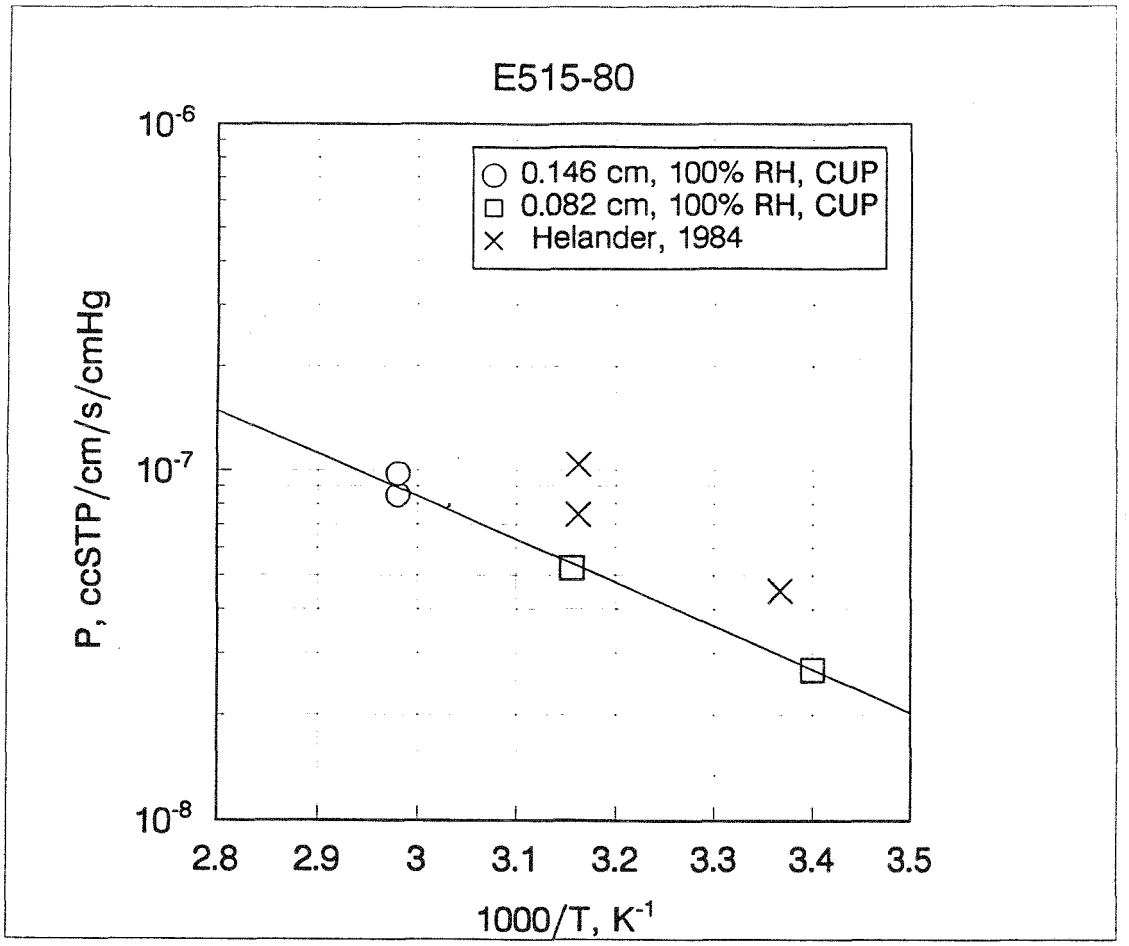

Figure 7. Permeability coefficient results for the E515-80 material plus literature values plotted versus inverse absolute temperature.

permeation cup method, we could not get repeatable results at temperatures of 50°C or below for this material, even using our thinnest samples (~0.07 cm thick). The reason was clear from the infrared results, since the low P value found at room temperature would correspond to a weight loss of ~ 1 mg/month for a water-filled cup sealed with a 0.07 cm thick B612-70 sample. Since our typical scatter for a given measurement was ~ ±1-2 mg (see Fig. 1), it would be impossible to measure such low permeability coefficients using permeability cups. As usual, literature values scatter over a wide range. Previous permeation cup measurements (Helander, 1984) made on the identical formulation (B612-70) are shown on Fig. 10, even though we question the author's ability to accurately measure the claimed 1 mg weight change in his 16 day room temperature run since his results typically show more scatter (many mg) from the weight loss lines than ours do. Also plotted on Fig. 10 are older results for an uncrosslinked, unfilled butyl gum stock (Morgan, 1953) and an unspecified formulation (Allen, 1977) which are higher than our results, a more recent room-temperature result (Rogers, 1985)

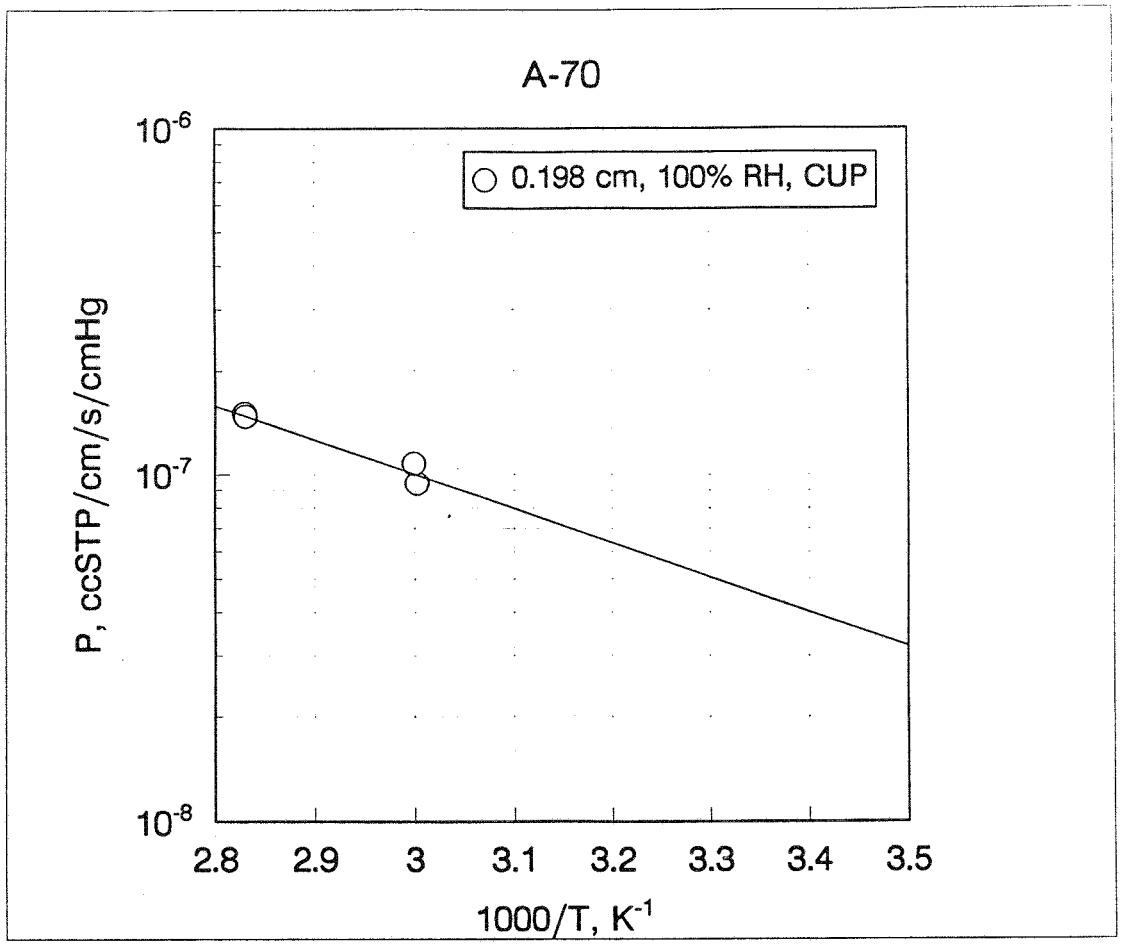

Figure 8. Permeability coefficient results for the A-70 material plotted versus inverse absolute temperature.

which is in excellent agreement with our value, and results (Doughty, 1981) which are even lower at room temperature but agree with our results at slightly elevated temperatures. Although it is clear that the final word has not been spoken on butyl's water permeability coefficients, it is apparent that, whatever the real values are, butyl rubber is an excellent material for sealing out water vapor.

At the opposite extreme are the silicone and fluorosilicone materials which are among the worst choices for sealing out water vapor. Figure 11 plots our permeation cup results plus our 35°C sorption/desorption results for the three materials included in the current study; as before, the results from the two methods agree within the estimated experimental uncertainties. In addition, our results are in accord with typical literature values (Barrie and Machin, 1969; Helander, 1984). The activation energies E_a (eq. 7) for our fluorosilicone materials are near zero and the E_a for our silicone is negative (-1.6

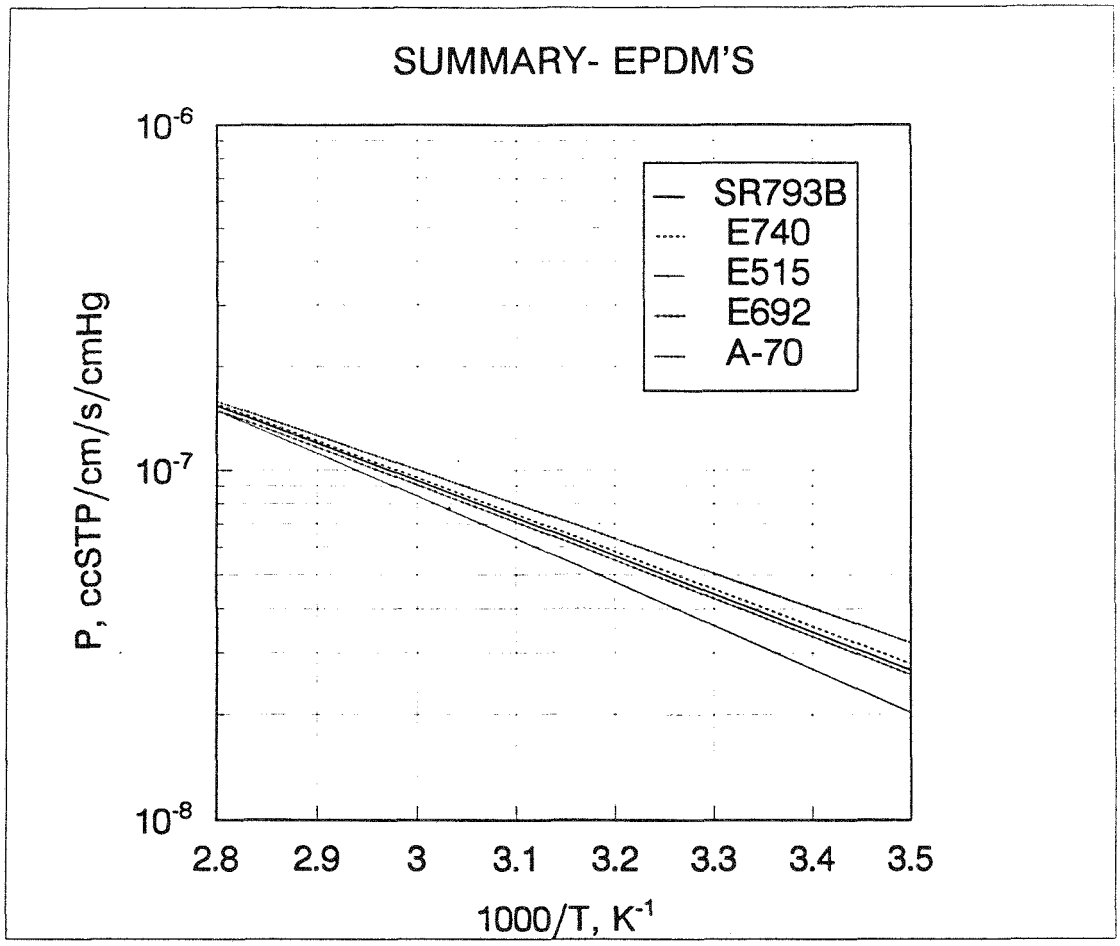

Figure 9. Summary of our permeability coefficient results for the five EPDM materials.

kcal/mol). Although these results may appear unusual, similar behavior has also been found for these materials in the literature (Barrie and Machin, 1969; Helander, 1984).

CONCLUSIONS

We have used three different experimental techniques in order to derive values of the water permeability coefficients for several different elastomeric formulations which have been used or are being considered for use as environmental seals in various past, present and future weapon systems. Included were five EPDM materials (E740-75, E515-80, E692-75, SR793B-80 and A-70), a butyl rubber material (B612-70), two fluorosilicone materials (S041-70 and LS-53) and a silicone rubber material (S604-70). Measurements were generated at relative humidities ranging from 75% to 100% and temperatures from ~21°C to 80°C. Data from the various techniques were in reasonable agreement and allowed us to obtain estimates of the Arrhenius activation energies for the permeability coefficient. Table 5 summarizes the results for the lines drawn through the

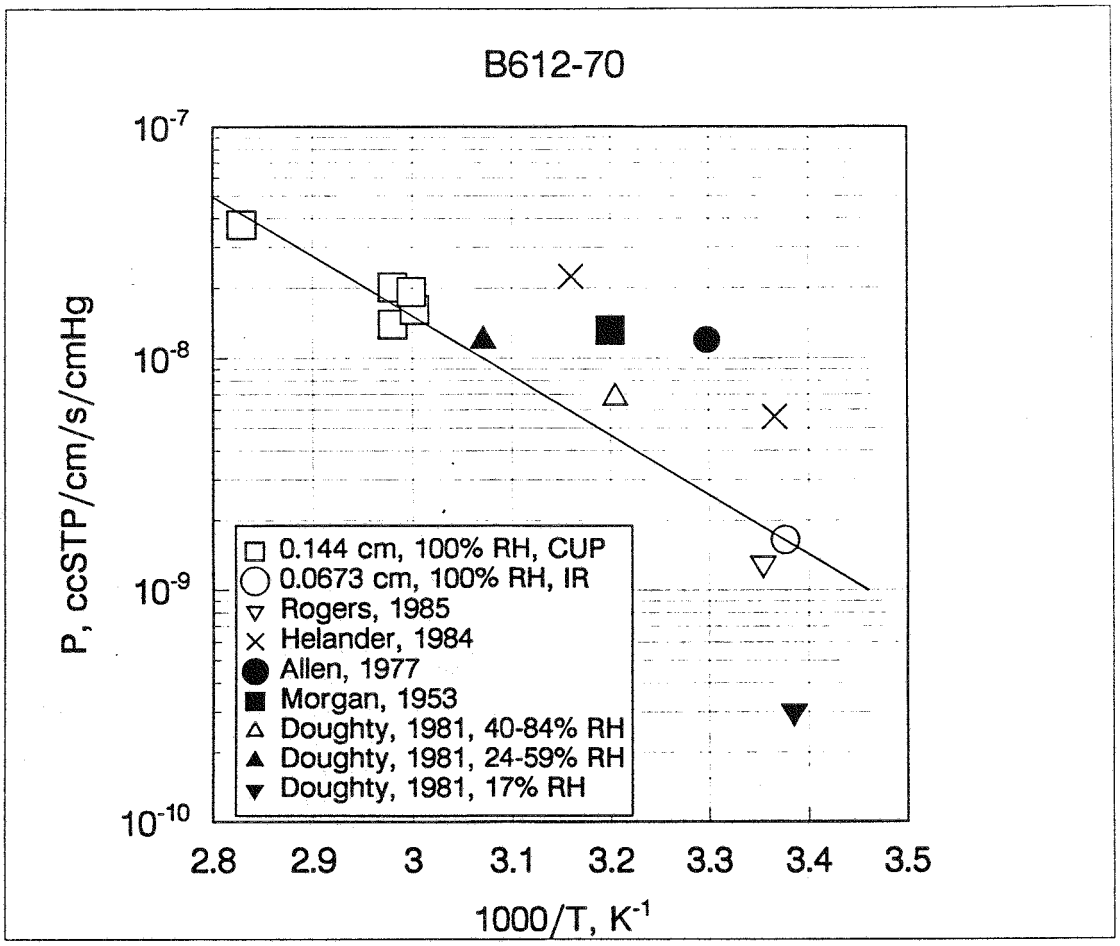

Figure 10. Permeability coefficient results for the B612-70 material plus literature results plotted versus inverse absolute temperature.

data on Figs. 4-11. The permeability coefficient results generated in this study will allow better estimates to be made of the lifetime quantity of water which permeates into a particular weapon.

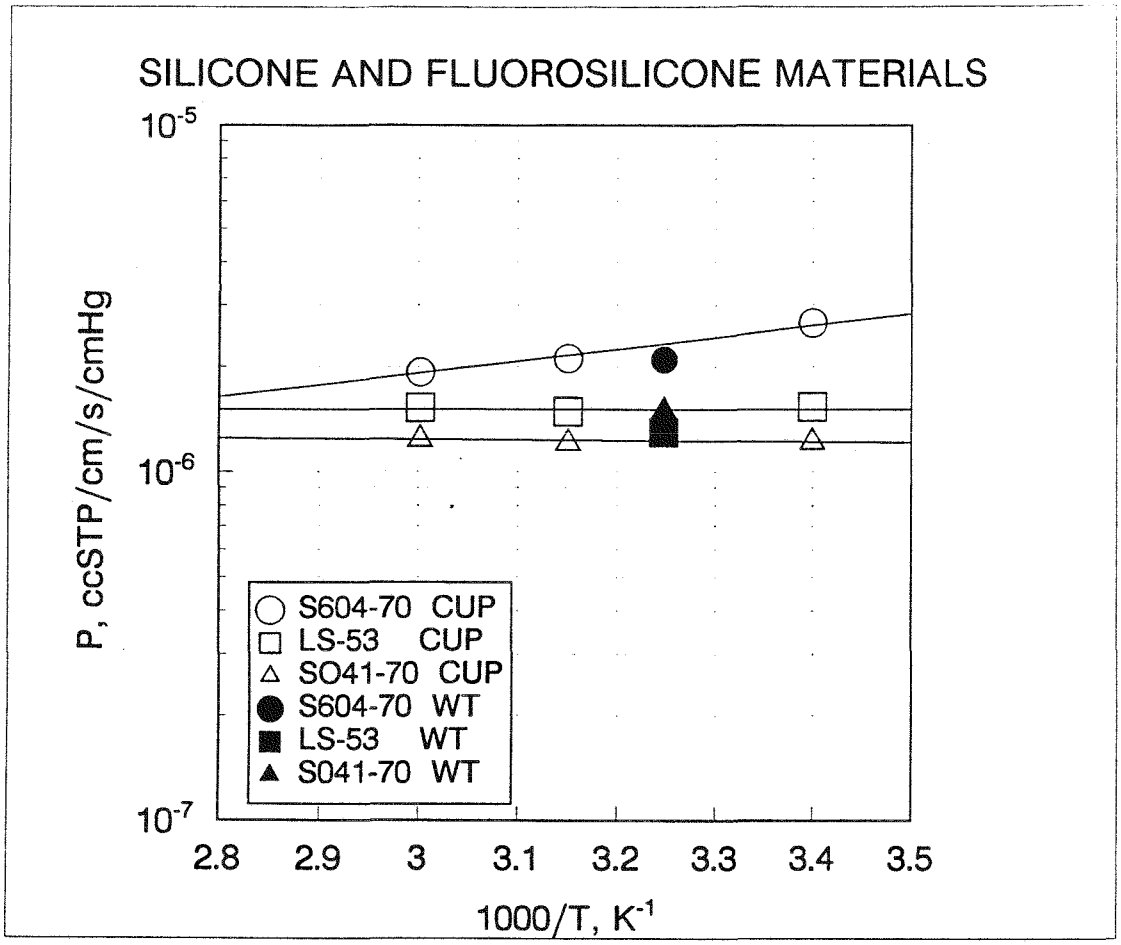

Figure 11. Permeability coefficient results for our silicone and fluorosilicone materials plotted versus inverse absolute temperature.

Table 5. Summary of Water Permeability Coefficient Results

Compound Number	Polymer Type	P at 25°C ccSTP/cm/s/cmHg	E_a kcal/mol
B612-70	Butyl	1.88E-9	11.8
E740-75	EPDM	4.0E-8	4.88
E515-80	EPDM	3.08E-8	5.66
E692-75	EPDM	3.75E-8	4.97
SR793B-80	EPDM	3.86E-8	4.96
A-70	EPDM	4.48E-8	4.55
S604-70	Silicone	1.79E-6	-0.31
LS-53	Fluorosilicone	1.51E-6	0
S041-70	Fluorosilicone	1.22E-6	0.08

REFERENCES

Abrams, A and G. J. Brabender (1936), "Factors Affecting the Determination of Water Vapor Permeability", Paper Trade Journal *102*, 32-41.

Allen, S. M., M. Fujii, V. Stannett, H. B. Hopfenberg and J. L. Williams (1977), "The Barrier Properties of Polyacrylonitrile", J. Mem. Sci., 2, 153-164.

Barrie, J. A. and D. Machin (1969), "The Sorption and Diffusion of Water in Silicone Rubbers. Part I Unfilled Rubbers", J. Macromol. Sci., Phys., *B3*, 645-672.

Barrie, J. A. (1968), "Water in Polymers", Ch. 8 in **Diffusion in Polymers**, J. Crank and G. S. Park, Eds., Academic Press, London.

Comyn, J. (1985) "Introduction to Polymer Permeability and the Mathematics of Diffusion", Ch. 1 in **Polymer Permeability**, J. Comyn, Ed., Elsevier Applied Science, London.

Crank, J. (1975), **The Mathematics of Diffusion**, 2nd Edition, Clarendon Press, Oxford

Doughty, D. H. (1981), "Water Vapor Permeation through Organic Materials", Sandia National Laboratories Report SAND81-8250.

Gillen, K. T. (1987), "A Better Method for Estimating Long-Term Ingress of Water into weapons Based on Argon Gas Concentration", Sandia National Laboratories Report SAND87-0809.

Gillen, K. T. (1990), "Argon Gas Analysis to Predict Water Leakage in the W88", Sandia National Laboratories Report SAND90-1852.

Helander, R. D. and W. B. Tolley (1984), "Water Vapor Transmission Rate (WVTR) of Elastomeric Materials", 29th National SAMPE Symposium.

Morgan, P. W. (1953), "Structure and Moisture Permeability of Film-Forming Polymers", Ind. Eng. Chem., *45*, 2296-2306.

Newns, A. C. (1950), "The Methods of Determining the Water Vapor Permeability of Laminae. A Review of the Literature", J. Textile Inst., *41*, T269- T308.

Parker (1982), **Parker O-Ring Handbook**, Parker Seal Group, Lexington, Kentucky.

Rogers, C. E. (1985), "Permeation of Gases and Vapours in Polymers", Ch. 2 in **Polymer Permeability**, J. Comyn, Ed., Elsevier Applied Science, London.

DISTRIBUTION

Gene Mortenson, C920
Los Alamos National Laboratory
Los Alamos, NM 87545

Jim Lemay
Lawrence Livermore National Laboratory
P. O. Box 808, Mail Stop L-322
Livermore, CA 94550

Allied Signal Aerospace Co. (3)
Kansas City Division
Attn. Erich Grotheer
Mike Smith
Mark Wilson
P. O. Box 419159
Kansas City, MO 64141-6159

0361 J. L. Duncan
0361 C. L. Sparks
0363 J. N. Middleton
0363 F. P. Freeman
1800 A. D. Romig
1811 R. L. Clough
1811 C. Arnold
1812 C. L. Renschler
1812 R. A. Assink
1812 K. T. Gillen (20)
1823 J. A. Borders
1824 M. R. Keenan
1845 P. F. Green (10)
1846 D. H. Doughty
2472 J. A. Sayre
2472 R. L. Myers
2472 K. B. Wischmann
5111 W. J. Patterson
5115 J. O. Harrison
5151 J. D. Brozek
5151 R. E. Davis
5153 S. L. Jeffers
5154 R. L. Alvis
5202 D. J. Bohrer
5203 C. C. Burks
5354 C. W. Pretzel
5361 M. H. Reynolds

5362 C. A. Pura
5363 D. J. Beyer
5363 J. D. Huntting
5365 G. C. Story
5366 A. C. Skinrood
5366 R. B. Anderson
7141 Technical Library (5)
7151 Technical Publications
8523-2 Central Technical Files
8700 R. C. Wayne
8711 J. E. Costa
8713 R. W. Bradshaw
8714 M. W. Perra
8716 R. E. Stoltz
7613-2 Document Processing for DOE/OSTI (10)